Author(s): Leppänen, Ari-Pekka; Peräjärvi, Kari; Paatero, Jussi; Joutsenvaara, Jari; Hannula, Antti; Hepoaho, Arttu; Holm, Philip; Ilander, Tarja; Kärkkäinen, Jouni

Title: Thunderstorm ground enhancements in Finland : observations using spectroscopic radiation detectors

Year: 2024

Version: Published version

Please cite the original version:

Leppänen, A.-P., Peräjärvi, K., Paatero, J., Joutsenvaara, J., Hannula, A., Hepoaho, A., Holm, P., Ilander, T., & Kärkkäinen, J. (2024). Thunderstorm ground enhancements in Finland : observations using spectroscopic radiation detectors. Acta Geophysica, Early online. https://doi.org/10.1007/s11600-024-01495-0

Acta Geophysica
https://doi.org/10.1007/s11600-024-01495-0

RESEARCH ARTICLE - ATMOSPHERIC & SPACE SCIENCES

Thunderstorm ground enhancements in Finland: observations using spectroscopic radiation detectors

Ari-Pekka Leppänen[1,5] · Kari Peräjärvi[1,4] · Jussi Paatero[2] · Jari Joutsenvaara[3] · Antti Hannula[1] · Arttu Hepoaho[3] · Philip Holm[1] · Tarja Ilander[1] · Jouni Kärkkäinen[1,6]

Received: 13 May 2024 / Accepted: 14 November 2024

Abstract
This study reports observations of Thunderstorm Ground Enhancements (TGE) that occurred in Southern Finland in the Municipality of Vantaa (60° 18' N 24° 58' E at 55 m a.m.s.l) on May 17th, 2020 between 10:23 and 10:28 UTC. The TGEs occurred when a storm front moved across the Helsinki region from roughly a southwest to northeast direction. The TGEs were caused by a Runaway Relativistic Electron Avalanche (RREA) occurring inside a thundercloud. Three independent measuring units of high-volume NaI(Tl) γ spectrometers were used to record ambient dose rate and γ spectra. The observed TGEs manifested themselves as sudden increases in γ radiation on the ground with a wide range of energies from 100 keV up to the maximum of the detector system of 8.8 MeV. The first event lasted 50 s and produced an increase in γ radiation of about 7–12% in the spectra measured with a ten-second collection time. The enhancement in γ radiation was terminated suddenly and simultaneously with an in-cloud lightning strike. This was followed by an 88–100 s long period when the level of γ radiation returned to normal values. After this, a second enhancement was observed to increase the level of γ radiation by 20–50%. The second enhancement lasted 100 s and it was also terminated simultaneously with an in-cloud lightning flash. The second enhancement appears to be stronger, but the exact locations of the thundercloud emitting the γ radiation were not known. From the duration of the second enhancement and the prevailing wind speed, the size of the RREA was estimated to be 400–1000 m. In the second enhancement, the most intense increase was between 100 and 1000 keV, although very-high-energy γ rays was observed up to 8.8 MeV. The shape of the background-subtracted γ spectra agreed well with the observations and predictions of the shape of the bremsstrahlung spectrum emitted by an RREA. Additionally, in the background-subtracted spectra, a minor enhancement of the 511 keV peak was also observed where the RREA also increased the number of positrons which annihilated and increased the emission of the 511 keV γ rays. The results of these high-latitude, low-altitude TGE events are the first ones report in Finland.

Keywords Terrestrial ground enhancement · Relativistic runaway electron avalanche · γ radiation · Thunderstorm · Finland

Introduction

The first discovery of the emission of γ radiation from thunderclouds was made by the BATSE instrument on board the Compton Gamma Ray Observatory (CGRO) satellite in

Edited by Prof. Theodore Karacostas (CO-EDITOR-IN-CHIEF).

✉ Ari-Pekka Leppänen
ari-pekka.leppanen@ec.europa.eu

[1] Radiation and Nuclear Safety Authority, Jokiniemenkuja 1, 01370 Vantaa, Finland

[2] Finnish Meteorological Institute, P.O.Box 503, 00101 Helsinki, Finland

[3] University of Oulu, Pentti Kaiteran Katu 1, 90570 Oulu, Finland

[4] University of Jyväskylä, Survontie 9D, 40500 Jyväskylä, Finland

[5] European Commission, Joint Research Center, Hermann-von-Helmholtz-Platz 1, 76344 Eggenstein-Leopoldshafen, Germany

[6] University of Helsinki, Viikinkaari 11, 00014 Helsinki, Finland

Published online: 12 December 2024

the early 1990s. CGRO was designed to observe γ radiation from stellar objects, but it occasionally observed fast pulses of γ radiation which were too short to be produced by stellar objects. In the investigations, it turned out that the γ radiation pulses originated from tropical thunderclouds where upward directed lightning flashes created γ radiation pulses with energies of up to 20 MeV (Fishman et al., 1994, Smith et al. 2005). These events lasted on the order of a fraction of a millisecond, and were named Terrestrial Gamma Flashes (TGFs). Thus, it was discovered that thunderclouds can accelerate electrons to high enough energies to start emitting γ radiation.

The processes inside thunderclouds that can excite and create natural particle accelerator-like conditions have been studied since the early 1990s. Globally, approximately 8.6 million lightning strikes are detected in a day, while it has been estimated that around 50 thunderclouds per day produce favorable acceleration conditions for a TGE to occur (NWS, 2024). Hence, among thunderstorms, a TGE is a rather rare event. Moreover, since suitable radiation detector systems are typically in fixed locations, most TGE events go unnoticed. To study TGEs, the detector systems need to be relatively close to the charge center of a thundercloud. Observation stations at high altitudes on top of a mountain offer a great place to study the phenomena or, alternatively, observations can be made at sea level when the cloud base is at a low altitude for observations to be made from the ground. The observation stations at high altitudes or balloon-borne missions provide a good opportunity to even be inside a thundercloud and close to the charge center. Most of the TGE observations today are made from ground-based detectors either in high-altitude observation stations on mountains where the observation station is close to the charge center of a thundercloud. In mountains stations, most of the TGE are observed during spring and fall (Kolmašová et al. 2022; Chilingarian 2023). The sea level observations are mostly done during winter storms where the cloud base is close to ground level making the observations possible (Chubenko et al. 2000; Torii et al. 2002, 2009; Gurevich et al. 2011; Wada et al. 2019). In some cases, RREAs and γ-ray emissions inside a thundercloud have been observed with detectors onboard airplanes and balloons (Parks et al. 1981; Eack et al. 1996; Helmerich et al. 2024).

In 1925, C.T.R. Wilson discovered the runaway electron mechanism in which fast electrons may obtain large energies from static electric fields in the air (Wilson 1925). Runaway electrons are produced in the air when the energy gained from the electric field exceeds the losses from collisions, allowing the electrons to accelerate to relativistic energies. An avalanche of such runaway electrons develops when energetic knockoff electrons are produced via hard elastic (Møller) scattering with electrons in the air molecules. These knockoff electrons subsequently runaway, producing more energetic knockoff electrons (Dwyer 2003). These runaway electrons together create a cascade, which is known as Relativistic Runaway Electron Avalanche (RREA). The RREA is a threshold process that occurs only if the atmospheric electric field exceeds the critical value in a region with a vertical extent of 1–2 km. The threshold (critical) energy steadily increases with increasing in air density according to $E_{th} = 2.18 \times 10^5$ V/m*n, where n is the relative air density (Dwyer 2003 and references therein). High-energy cosmic rays entering into Earth's atmosphere produce particle showers, exotic particles and above all atmospheric ionization (Bazileskaya 2008; Usoskin and Poluianov 2024 and references therein). Atmospheric ionization produces the initial free electrons that can be accelerated and multiplied in number in the strong electric inside a thundercloud leading to a runaway process.

Experiments conducted between 1945 and 1949 at the Zugspitze Geodynamic Observatory in Germany revealed a rather complex structure of the intracloud electric fields. In some thunderclouds, Joachim Küttner discovered a pocket of positive charge at the base of a thundercloud, which was named the lower positive charge region (LPCR) (Küttner 1950). In a simplified thundercloud tripole structure, there are three main charge regions: a positive charge region at the top of the cloud and the main negative charge region in the middle and a relatively small LPCR at the bottom, close to the base of the cloud. The thundercloud tripole structure is a prerequisite for a TGE. In Japan, short-lived tripole structures are thought to appear in winter thunderstorms. In winter thunderstorms, the cloud base is close to ground level making the detection of TGEs possible. Sometimes, the TGEs are also referred to as terrestrial gamma glows (TGGs) since the RREA lasts of the order of tens of seconds to minutes making the cloud "glow" γ rays (Wada et al. 2019; Hisadomi et al. 2021). In mountain observation stations, enhancements of particle fluxes have been detected in conjunction with the emission of γ rays (Chilingarian 2014; Kolmašová et al. 2022). Hence, in TGE observatories, γ rays and electron fluxes can be measured simultaneously. The possibility to observe TGEs with γ-ray and electron enhancements is higher in spring and in autumn when the cloud base, and the LPCR, is closer to the ground level. In summer, the cloud base height is typically higher and only γ rays reach Earth's surface but not the electrons (Chilingarian 2023).

The γ rays produced in an RREA have a wide range of energies ranging from a few tens of keVs up to several tens of MeVs. In RREA-induced terrestrial gamma flashes, γ rays with energies of up to 50 MeV have been observed (Marisaldi et al. 2010). In the TGEs reported in the literature, the observed γ ray spectrum has a power law shape where the intensity drops as a function of energy. The highest intensities are observed at low energies around 100 keV, while

the very high-energy γ rays with energies of several MeVs have low intensities (Chilingarian et al. 2022). The TGEs and TGFs can locally increase the ionizing radiation fields, which, in turn, can cause increased radiation doses to flight crews and airplane passengers and can harm airplane avionics (Maia et al. 2024; Tavani et al. 2013).

Furthermore, recent studies have suggested that RREAs can also induce secondary nuclear reactions by exciting the atmospheric nitrogen and oxygen nuclei. These reactions have been seen as an enhancement in the 511 keV annihilation peak where the 511 keV peak enhancement has been delayed after the TGE. The energy of the γ rays is high enough to trigger atmospheric photonuclear reactions, thus producing neutrons and eventually positrons via $\beta+$ decay of the unstable radioactive isotopes. In such a case, the atmospheric photonuclear reactions $^{14}\mathrm{N}+\gamma\rightarrow{}^{13}\mathrm{N}+\mathrm{n}$ and $^{16}\mathrm{O}+\gamma\rightarrow{}^{15}\mathrm{O}+\mathrm{n}$ generate fast neutrons with a kinetic energy of $E_0\approx10$ MeV and unstable ^{13}N and ^{15}O which decay gradually into stable ^{13}C and ^{15}N nuclei via β + decays. The positron ($\beta+$) gets annihilated when met with an electron via emitting two 511 keV γ rays (Enoto et al. 2017).

Many of the low-altitude observations have been made during the winter storms where the cloud-base altitude and the LPCR are relatively close to the ground compared to the summer storms (Torii et al. 2002, 2011; Enoto et al. 2017; Wada et al. 2019; Hisadomi et al. 2021). These conditions can also be met in high-latitude regions where cloud bases in spring and summer thunderstorms are typically lower compared to more southern latitudes. In high-latitude regions, thunderstorms are very rare during winter but relatively frequent during summertime. In Finland, 0.71% of the ground flashes occur from November to April and 99.29% occur from May to October (Mäkelä et al. 2014). Even though wintertime lightning strikes are rare, they can cause significant consequences (Mäkelä et al. 2013). In this study, we will discuss the observation of two TGE events that occurred in a high-latitude region outside the typical latitude region where TGE events have been reported before. The TGE events in this study occurred in Southern Finland in the Municipality of Vantaa on May 17th, 2020, around 13:20 local time when a strong storm front passed through the southern part of Finland and the capital region of Helsinki bringing lightning, rain and sleet.

Materials and methods

The Radiation and Nuclear Safety Authority (STUK) in Finland has multiple radiation detection systems for measuring environmental radioactivity. On May 17th, 2020, STUK was conducting γ spectrometric measurements in the Municipality of Vantaa (60° 18' N 24° 58' E at 55 m a.m.s.l.) located in Southern Finland, about 20 km north of the Finnish capital Helsinki. For a TGE event, this is a high-latitude and very low-altitude location. The measurements were done with three units of relocatable 4″ × 4″ × 16″ NaI(Tl) scintillation detectors, with each detector system working independently. In each detector system an NaI(Tl) detector was connected to a photo-multiplier tube (PMT) which was, in turn, connected to a Canberra Osprey digital multichannel analyzer (MCA) using 2048 channels (Holm et al. 2013). The 4″ × 4″ × 16″ NaI(Tl) detectors were high-volume detectors allowing the efficient detection of γ rays with a wide energy range. The high efficiency comes with a cost since the resolution of the NaI(Tl) detectors is normally poor compared to, for example, CdZnTe or HPGe detectors. The different detector systems used here were labeled as Detectors 1, 2 and 3. The detector systems recorded γ-ray spectra with time information in two modes: two seconds and ten seconds. The recorded γ-ray energy range extended from 130 keV up to about 8.8 MeVs allowing the detection of very high-energy γ rays. In environmental γ spectrometry, the γ rays with energies above the ^{208}Tl 2614.5 keV peak are very rare, and the only source for γ rays above 3 MeV in energy is the bremsstrahlung from cosmic ray muons, but this flux is low and relatively steady. This makes any enhancement in the high-energy region particularly interesting. The detector systems also calculated the dose rate but they will not be discussed here since the conversion of hard γ rays to accurate dose rate values is difficult and contains large uncertainties. The detector systems operated independently where Detectors 1 and 2 were about 150 m apart, and Detectors 2 and 3 were about 100 m away from each other forming roughly an L-shaped pattern. The measured spectra were saved into a common data storage system together with time marked in Universal Time Coordinates (UTC). It should be noted that the local time in Finland is UTC + 3 h during daylight saving time from the end of March to the end of October.

Meteorological observations with a one-minute frequency were obtained from the nearby aviation weather station at the Helsinki-Vantaa Airport operated by the Finnish Meteorological Institute (FMI). The weather measurements are carried out according to specifications by the World Meteorological Organization (WMO) and the International Civil Aviation Organization (ICAO). The lightning data were obtained from the FMI's nationwide lightning observation network. Lightning strikes are detected by their radiofrequency emissions. The positioning is based on the signal arrival time to different sensors in the network and peak current estimation on the signal amplitude. In the Helsinki area, the location error is usually 200–300 m (Mäkelä et al. 2017). Wind observations 327 m above ground were obtained from Espoo Latokaski television/radio mast, 25 km SW of the study area, where the FMI measures meteorological parameters at several heights.

Data analysis

Weather at Vantaa during 09:00–12:00 UTC

The weather one hour before the TGG was quite typical for the middle of May with no significant weather conditions: air temperature + 9 °C, relative humidity 53%, pressure 996 mbar, visibility 50 km, wind speed 3 m/s and direction 200°, cloud base at 1140 m above the ground and the tropopause height 7600 m above the ground level. Around 09:50 UTC, the storm front started to approach. The temperature began to drop from + 9.4 °C. The wind speed had increased from 3 to 5.5 m/s half an hour earlier, but the wind direction was more or less the same at 180°. Light rain started at 10:07 UTC and the wind speed was 4.4 m/s with a direction of 170°, the visibility had dropped to 8 km. At 10:16 UTC light rain had already turned into heavy rain and the wind speed was 8 m/s and the direction had turned almost to the opposite direction to 350°. At 10:19 UTC, the heavy rain turned into wet snow and the temperature had dropped to + 2.9 °C, a drop of 7 °C in a half an hour, and the visibility had reduced to 800 m. At 10:23 UTC, the time of the first TGE event, the cloud base had dropped to 640 m above ground level and the temperature had dropped to + 2.6 °C. Snowing started with medium intensity, the wind speed was 6.7 m/s and in the direction of 320°. Due to the rain and snow, the relative humidity had risen to 89%. At 10:26–10:27 UTC, during the second event, the weather parameters were the same except the wet snow had turned into rain. There was a possible third TGE event at 10:28:48 UTC, during which the weather parameters were the same except the cloud base had dropped down to 520 m above ground level. The dropping of the cloud base to 500-600 m brought the LPCR close enough for the TGEs to be observed.

The weather parameters are plotted in Fig. 1 Panels A-E. One of the most interesting weather parameters was the global radiation as shown in Fig. 1 Panel F. Before the TGG event, the global radiation varied largely between 150 and 1100 W/m^2 depending on the random cloud cover. However, from 10:00 UTC to about 10:30 UTC, the level of the global radiation decreased from 1068 W/m^2 to 7.9 W/m^2 within half an hour. The cloud cover was, for a moment, optically so thick that it absorbed over 99% of solar radiation. This means that the cloud emitting γ radiation also contained large amounts of moisture and cold air, making the cloud in this storm front exceptional in many ways. It should also be noted that the storm front arrived at Vantaa from the southwest over the Gulf of Finland. Hence, before arriving at Vantaa, the storm front had spent a significant amount of time above the Baltic Sea increasing its moisture content.

Timing of the TGE events

Connected to the severe weather conditions, lightning flashes were observed and recorded by FMI's lightning observation network. Lightning observations are important since

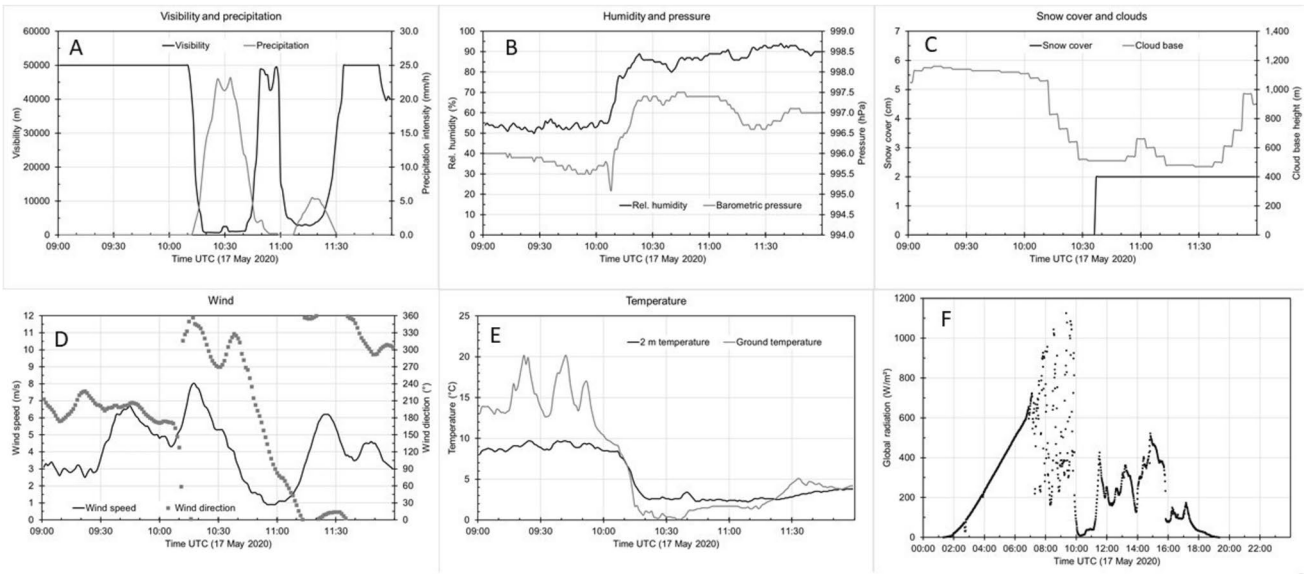

Fig. 1 Weather parameters from the Helsinki-Vantaa airport from 09:00 to 12:00 UTC. Panel A shows the barometric pressure (gray) and relative humidity (black). Panel B shows the cloud base in meters above the ground (gray) and the snow cover (black). Panel C shows the visibility (black) and the precipitation intensity (gray). Panel D shows the ground level temperature (gray) and the 2 m air temperature (black). Panel E shows the temperature at ground level (gray) and the temperature at 2 m altitude (black). Panel F shows the global radiation

the TGEs are typically terminated by an in-cloud discharge between the main negative charge region and the LPCR. This ends the RREA process since the atmospheric electric field has dropped below the critical value beyond which no more acceleration of electrons is possible (Dwyer 2003).

Figure 2 shows the location of the flashes observed during 10:16 and 10:31 UTC. The blue circles indicate the locations of the lightning that hit the ground and the red circles indicate in-cloud discharges. The red triangle indicates the location of the detectors. There are a number of in-cloud discharges around the locations of the detectors–numbers 10, 13, 19, 21, 22, 24 and 33 that can be considered as candidates that ended the RREA and stopped the TGE events.

From the locations of the lightning strikes and the measured wind direction, it can be estimated that the thundercloud causing the TGE was very close to or possibly even at some point directly above the detectors.

Figure 3 shows the time series of the total number of counts in the 10 s. spectra collected in all three detectors. The total number of counts represents the amount of radiation seen by the detector throughout the whole energy of the detector. Unfortunately, the Detector 1 suffered from stability issues where the baseline jumped up and down during collection producing sporadic spikes in the count rate time series. The count rates in Detectors 2 and 3 were stable throughout the study period. In Detectors 2 and 3, the count rate baseline slightly increased after the TGE events. This was most likely caused by the washout of short-lived radon progeny from air to ground after intensive rain and snowfall (Paatero and Hatakka 1999). The x-axis of Fig. 3's lower panel highlights the time period 10:17–10:33 UTC when the two or three γ radiation enhancements were observed. Detectors 1 and 3 both observed two events, while Detector 2 shows there was possibly also a weak third event.

In Fig. 3, the normal background varied between the detectors. In Detector 1, the background count rate was between 16,000 and 17,000 counts per 10 s., while in Detector 2, the background count rate was about 25,000 counts per 10 s., and in Detector 3, the background level was around 20,500 counts per 10 s. The count rate was dependent on

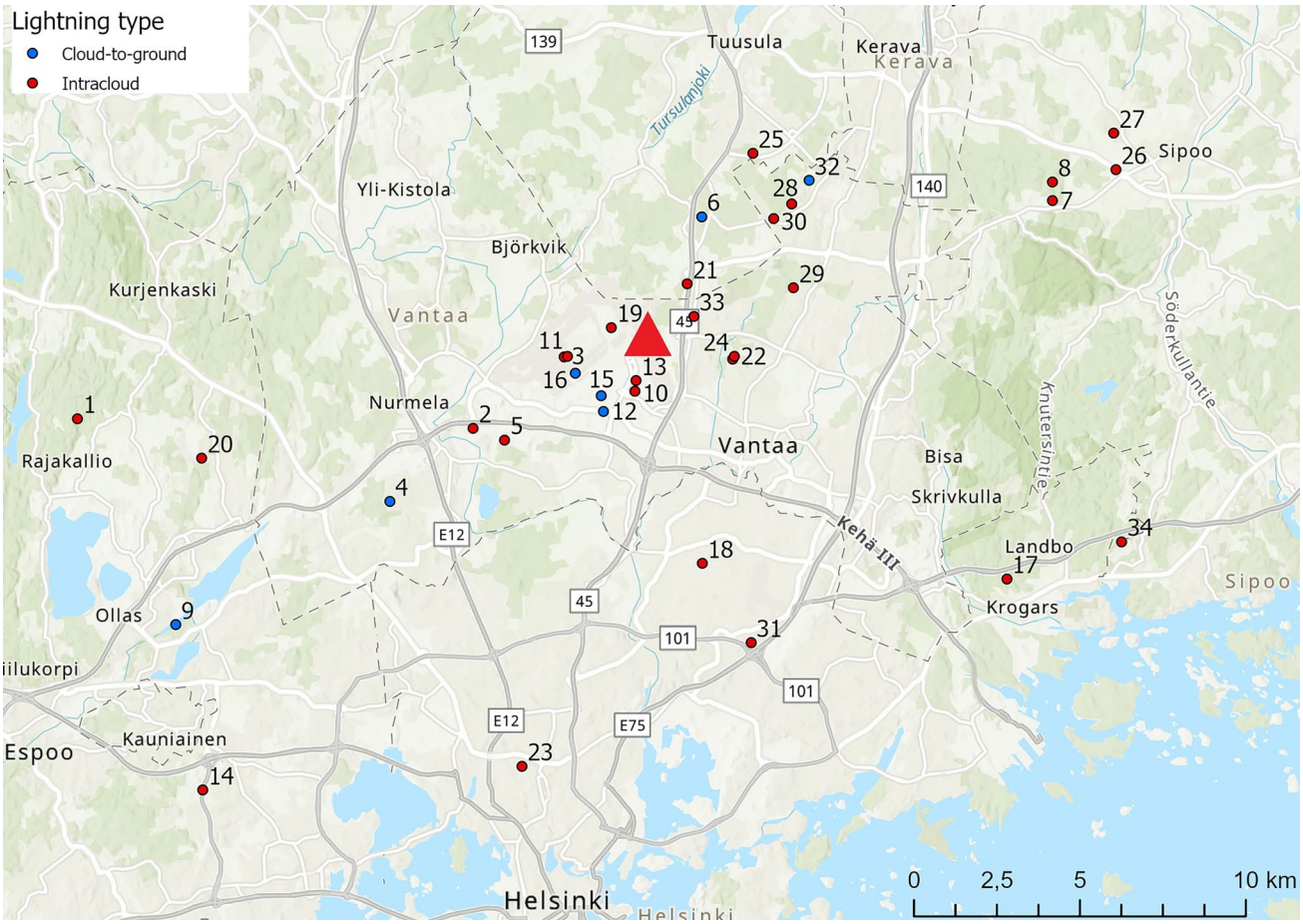

Fig. 2 Location of lightning strikes (circles) and the detector (triangle). Lightning strikes from cloud to ground are marked with blue and in-cloud lightning with red. The numbers refer to lightning numbering in Table 2. Base map data sources: Esri, Intermap, NLS, NMA, USGS; National Land Survey of Finland, TomTom, Garmin, Foursquare, METI/NASA

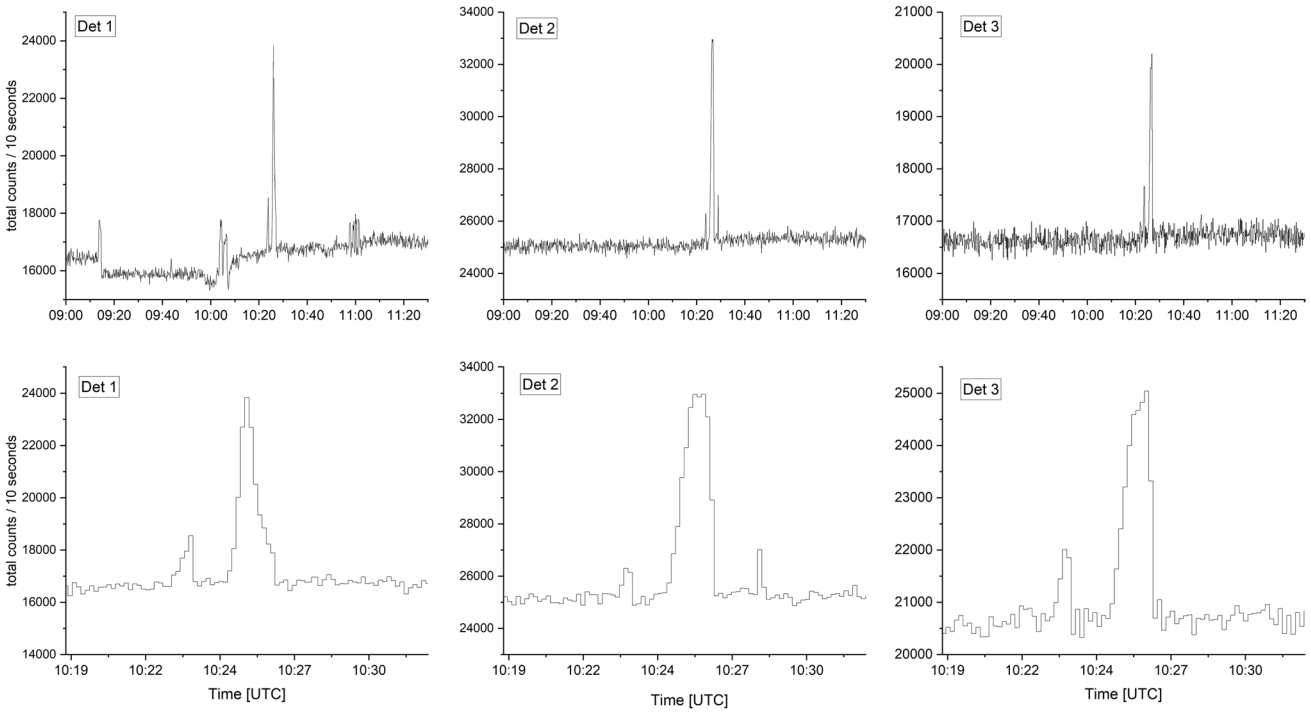

Fig. 3 Time series of the total number of counts in the spectra measured with 10 s time intervals

the detector location. The count rates were quite high due to the large volume of the detectors and due to the fact that the detectors were unshielded. As seen in the lower panels of Fig. 3 between 10:22 and 10:28 UTC anomalously, high count rates were observed in all three detectors simultaneously. This suggests the presence of a spatially larger source of radiation and rules out a point source. Compared to the trends of each detector, the observed increases in the total number of counts were too large to be caused by the random variation of background, but an actual source of radiation had to be present.

The first event was visible in all three spectra although the starting time varied slightly. The different starting times can be explained by the placement of the detectors. The detectors were placed some hundred meters apart and thus the cloud emitting γ rays triggered the detectors at slightly different times. In the first event, the total number of counts in 10 s. spectra in the Detector 1 increased from roughly 16,500 to 18,500 counts, making the increase in the count rate of about 12%, in Detector 2, the increase was from 25,100 to 26,300 counts corresponding to an increase in approximately 5% and in Detector 3, the increase was from 20,600 to about 22,000 counts with an increase in about 7%. After the first event, the count rates in all detectors dropped rapidly in a matter of seconds to the background level and remained there for about 80–90 s. After this, much larger increases were observed in all three detectors. In Detector 1, the total count increased from approximately 16,500 to 24,000 counts corresponding to an increase in about 45%. In Detector 2, the second event raised the total count number from about 25,000 to 33,000 corresponding to an increase in about 31%, and in Detector 3, the total count number increased from about 20 700 to 25 000 corresponding to an increase in approximately 21%. The relative increases would suggest that Detector 1 was closest to the source of the second enhancement, and Detector 3 was the farthest. The time series of Detector 2 suggests a possible third, small event 100 s after the second event. This was not seen by the other detectors. This third event occurred at 10:28:48 UTC, and it was only visible in the 10 s. measurements. The total count number in Detector 3 increased from 25,300 to 27,000 corresponding to an increase in 7%. However, since this enhancement was not seen by other detectors and there was no lightning flash related to the termination, this enhancement remains as speculative and we will not discuss it further.

Information collected about the observed enhancements are presented in Table 1. The studies by Hisadomi et al. (2021) were inserted in the table for comparison. The γ-ray enhancements observed in this study and in Hisadomi et al. (2021) had very similar temporal patterns. Hisadomi et al. (2021) first observed a smaller enhancement which lasted ~ 30 s. with a sudden termination, and then, after a break of ~ 90 s., they observed a second and much larger enhancement lasting ~ 70 s. In the present study, the first enhancement lasted for ~ 50 s. with a sudden termination,

Table 1 The data of the TGEs reported in this study compared with two previously reported TGEs

	Increase 1st TGE*	Duration** [s]	Break [s]	Increase 2nd TGE	Duration [s]	Break [s]	Increase 3rd TGE	Duration [s]
Det 1	12%	48	88	40–50%	100			
Det 2	5%	Unknown	Unknown	30%	100	100	7%	~20
Det 3	7%	~50	100	20%	90			
Hisadomi et al. (2021)	Fourfold	30	90	Tenfold	70			

*The radiation increases were calculated from the spectra with a 10 s. collection time

**The duration and the break were determined from the spectra with a 2 s. collection time except the third event duration was determined from the spectra with a 10 s. collection time

and then a break of about 80–90 s. followed by a second and stronger event lasting ~ 100–130 s. Hence, the similar temporal pattern in both cases has been first, a weaker enhancement with sudden termination followed by a break for several tens of seconds during which the radiation levels drop to background level and after that a much stronger enhancement lasting several tens of seconds ending with a sudden termination.

Figure 4 Panel A shows the time series of the total number of counts above the background level in all three detectors with a two-second collection time. The background was estimated for Detector 1 as 3340 counts/2 s., for Detector 2, as 5030 counts/2 s. and for Detector 3 as 4130 counts/2 s. These background count rates were then subtracted from the time series to obtain Fig. 4A. Unfortunately, in two-second measurement, there were a lot of missing data points due to problems with the data storage. From these spectra, we can extract more accurate information on timing and the duration of the enhancements. The start times of the enhancements were decided when the count rate had risen above the count rate level of the maximum during the preceeding 1.5 h and vice versa for the ending time of the enhancement. The first enhancement was fully visible only in Detector 1 where the start of the enhancement was 10:23:12 UTC and the end time 10:24:00 UTC, making the total duration 48 s. During the first event, Detector 2 had only recorded one two-second spectrum and hence was omitted from the analysis. The data of Detector 3 start at 10:23:24 UTC when the count rate had already risen slightly above the background. The starting time in Detector 3 was estimated to be around 10:23:10 UTC and the termination time was 10:24:00 UTC making the total duration of the event approximately 50 s. The first event was terminated with a sharp cutoff at 10:24:00 UTC in both Detectors 1 and 3. The second enhancement started about 90 s. after the first enhancement. All three detectors recorded the second enhancement fully. In Detector 1 the starting time of the second enhancement was 10:25:28 UTC and the end time was 10:27:08 UTC, while in Detector

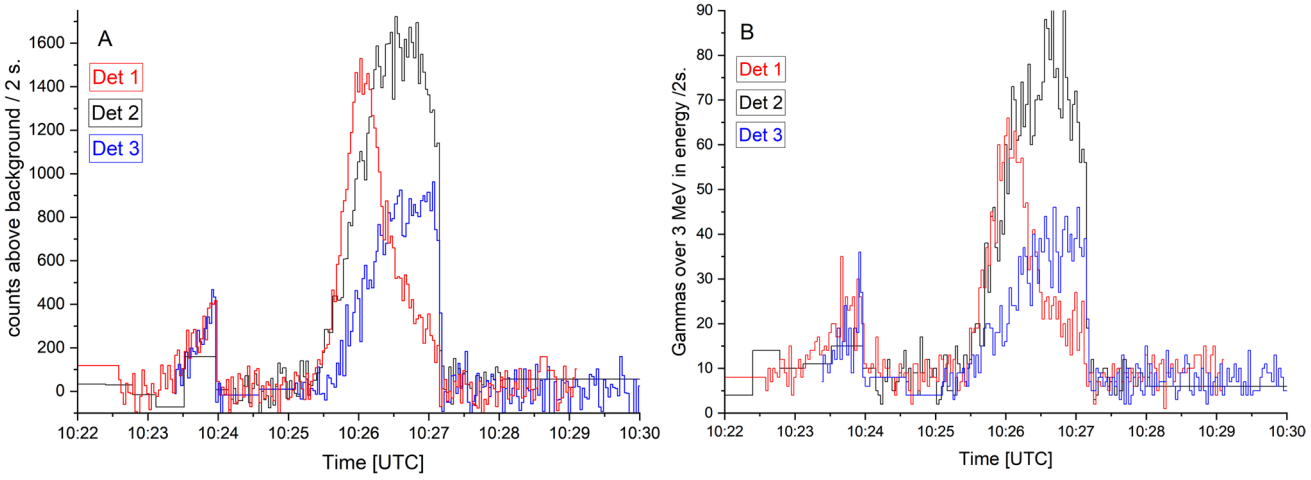

Fig. 4 Panel A: Time series of the background subtracted total counts in two-second spectrum from detectors 1, 2 and 3 drawn to common time scale starting from 10:22:00 to 10:30:00 UTC. Detector 1 data have shown in red, Detector 2 data have shown in black and Detector 3 data have shown in blue. Panel B: Time series of hard γ rays with energies above 3000 keV

2, the corresponding start and end times were 10:25:30 and 10:27:10 UTC, and in Detector 3 were 10:25:40 and 10:27:10 UTC, respectively. Hence, the duration of the second enhancement was 100 s. making it twice as long as the first one. The differences in starting times were most likely due to the different cloud-to-detector distances. The information about the enhancements is shown in Table 1

The temporal structures of the TGEs are revealing. The first enhancement shows a gradual increase where the count rates rise followed by a sudden termination. The second enhancement shows a similar temporal pattern in Detectors 2 and 3 with a relatively gradual increase in count rate then a peak phase and after that a termination with a very sharp cutoff. The temporal pattern, including the cutoff, was different in Detector 1. The second enhancement began at the same time in Detectors 1 and 2 but in Detector 1 the increase to the peak count rate was faster. The rise times of the second enhancement were 32 s., 66 s. and 44 s. in Detectors 1, 2 and 3, respectively.

The timing differences as seen in Fig. 4A and B can most likely be attributed to the different locations of the detectors and the movement of the cloud with respect to the detectors. The total count rate in Detectors 1 and 2 started to increase almost at the same time, while in Detector 3 the count rate began to increase about 14 s later. The movement of the thundercloud may have caused this where Detectors 1 and 2 might have been closer compared to Detector 3. After rising to the peak total counts in a spectrum, the total counts began to drop earlier in Detector 1 at 10:26:12 UTC which was about 44 s. earlier compared to Detector 2. Detectors 2 and 3 reached a brief steady phase where count rates were roughly stable before the sudden and sharp termination at 10:27:10 UTC. The peak phase in Detector 2 lasted 44 s. and in Detector 3 42 s. The temporal pattern in Fig. 4B was similar to that of Fig. 4A except the peaks in Detectors 1 and 3 during the second TGE were narrower. In Fig. 4B, the peak phase in Detectors 2 and 3 lasted roughly 50 s., from 10:26:10 to 10:27:00 UTC. Here, we refer to the γ rays with energies above 3000 keV as high-energy γ rays. High-energy γ rays are the best indicators of TGE since naturally occurring radionuclides (NOR) do not produce γ rays above 2700 keV. Figure 4 Panel B shows the high-energy γ rays during the TGE enhancements. The temporal behavior resembles the total γ rays shown in Fig. 4A even though the number of counts was reduced approximately by a factor of 25.

Table 2 shows the FMI lightning observations with a one-second time resolution. The table shows the calculated coordinates, multiplicity, i.e., how many strikes there were in one flash, the calculated peak current in kilo Amperes (kA) and the cloud indicator, which shows if the lightning struck from the cloud to the ground (0) or was an in-cloud (1) lightning. The lightning flashes marked in bold corresponded to the termination times of the TGEs. From Table 2 and Fig. 2, we can see that there were flashes around the study area. There were five flashes (numbers 17, 18, 19, 20 and 21) registered at 10:23:59 UTC which corresponds to the exact time of the termination of the first TGE. All five flashes were in-cloud discharges which are the requirement to discharge between the main negative and the LPCR. Flash number 19 had a relatively low peak current of 3 kA, but it is the closest one to our detectors and hence the candidate the most likely ended the first enhancement. The second enhancement was terminated at 10:27:10 UTC. The flashes number 22 and 24 were strong in-cloud discharges close to our detectors with high peak currents of 29 and 16 kA, respectively. Both Flashes 22 and 24 were downwind in respect to Flash number 19. The flash that ended the second TGE had about a ten times higher peak current compared to the flash that ended the first TGE. The recorded times of the in-cloud lightning flashes correspond exactly to the sharp terminations of the observed γ radiation enhancements. In the studies by Torii et al. (2011) and Hisadomi et al. (2021), the TGEs were terminated by in-cloud flashes. Mäkelä et al. (2017) reported that the median peak current of the flashes in 2016 was about 10 kA, but the most powerful ones exceeded 100 kA. Hence, the flashes that ended the second enhancement had significantly higher peak currents than a usual flash detected in Finland. As mentioned in the introduction, RREA is a threshold process requiring the electrical field to be above a certain threshold. When the potential drops below this threshold, the RREA and the TGE are terminated. The lightning flash discharges and drops the electric potential below the threshold value. This was seen as sudden termination of the two observed γ-ray enhancements by lightning numbers 19 and 22/24.

Horizontal size estimation of the γ-emitting region

Judging from the temporal behavior of the count rates in Detectors 2 and 3, as shown in Fig. 4A, there was a "peak phase" between 10:26:14 and 10:26:58 UTC when the γ-ray count rates had reached the peak values of 1400 counts/spectrum and remained relatively constant for about 42 s. This peak phase could represent the bottom of the LPCR, representing the area where the γ rays are emitted from. Here, the γ-ray emitting area passed close to Detectors 2 and 3 but Detector 1 data suggests it observed the edge or one side of the LPCR. The size of the γ-ray emitting area can be estimated by using the wind speed and the duration of the peak phase. The wind speed at the altitude of 327 m above ground (371 m a.m.s.l.) was, on average, 9.8 m/s between 10 and 11 UTC. Based on this and the duration of the peak phase in the second TGE event, 42–46 s, it can be estimated that the horizontal dimension of the LPCR causing the TGE was about 400–450 m. This concurs with the peak phase of the

Table 2 Finnish Meteorological Institute's lightning data before and after the two TGE events

Lightning ID	Longitude [°]	Latitude [°]	Time [UTC]	Cloud indicator	Multiplicity	Peak current [kA]
1	24,669	60,2955	10.16.52	1	1	3
2	24,8846	60,2965	10.16.52	1	1	9
3	24,9329	60,3165	10.16.52	1	1	12
4	24,8405	60,276	10.16.52	0	2	26
5	24,902	60,2936	10.16.52	1	1	7
6	25,0056	60,3556	10.16.52	0	1	–3
7	25,1967	60,3626	10.16.52	1	1	–3
8	25,1966	60,3677	10.16.52	1	1	–4
9	24,7263	60,2407	10.16.52	0	0	–4
10	24,9721	60,3079	10.18.55	1	1	18
11	24,9346	60,3168	10.18.55	1	1	5
12	24,9554	60,3022	10.18.55	0	1	35
13	24,9724	60,3107	10.21.52	1	1	22
14	24,7441	60,1963	10.21.52	1	1	–3
15	24,9538	60,3064	10.21.52	0	2	15
16	24,9393	60,3122	10.21.52	0	0	14
17	**25,1776**	**60,2601**	**10.23.59**	**1**	**1**	**9**
18	**25,0117**	**60,2619**	**10.23.59**	**1**	**1**	**3**
19	**24,9582**	**60,3249**	**10.23.59**	**1**	**1**	**3**
20	**24,7374**	**60,286**	**10.23.59**	**1**	**1**	**3**
21	**24,9989**	**60,3373**	**10.23.59**	**1**	**1**	**4**
22	**25,025**	**60,3173**	**10.27.10**	**1**	**1**	**29**
23	**24,9171**	**60,2056**	**10.27.10**	**1**	**1**	**3**
24	**25,0258**	**60,3181**	**10.27.10**	**1**	**1**	**16**
25	**25,0324**	**60,3731**	**10.27.10**	**1**	**1**	**5**
26	**25,2309**	**60,3715**	**10.27.10**	**1**	**1**	**–3**
27	**25,2293**	**60,3813**	**10.27.10**	**1**	**1**	**–3**
28	25,0545	60,3597	10.31.13	1	1	–6
29	25,0569	60,3371	10.31.13	1	1	–3
30	25,0448	60,3557	10.31.13	1	1	6
31	25,0395	60,2409	10.31.13	1	1	3
32	25,0636	60,3662	10.31.13	0	1	18
33	25,003	60,3286	10.31.13	1	1	6
34	25,2396	60,271	10.31.13	1	1	–3

The lightnings corresponding to the end of the TGE events are in bold

high-energy γ rays with energies above 3 MeV, as shown in Fig. 4B, which lasted about 50 s (10:26:12 -10:27:02). With the wind speed of 9.8 m/s, the size of the γ-ray emitting region can be estimated to be about 500 m. Furthermore, the upper limit can be estimated with the total duration of the second enhancements (10:25:32–10:27:12 UTC) which lasted about 100 s., hence, the upper limit for the horizontal size was about 1000 m. This size estimation agrees well with the size estimation of 700 m reported in Torii et al. (2011) but is significantly smaller than the cell of ~ 4 km reported in the study by Hisadomi et al. (2021). It should be noted that it is possible that we observed the thundercloud cell only partially and most likely the cell also had an internal structure where the γ-ray emissions were not emitted uniformly thus there could have been areas of higher and lower γ-ray fluxes. When considering emission from the LPCR to the ground, the high-energy γ rays scatter mainly in a forward direction at low angles and the angular spread from the cloud to ground is relatively small. This is also true for bremsstrahlung when the electrons have high enough energy to be treated relativistically, that is, the kinetic energy is as high as the rest mass of the electron (Köhn and Ebert 2014). This means that the area on the ground where γ rays are detected is comparable to the size of the LPCR inside the thundercloud.

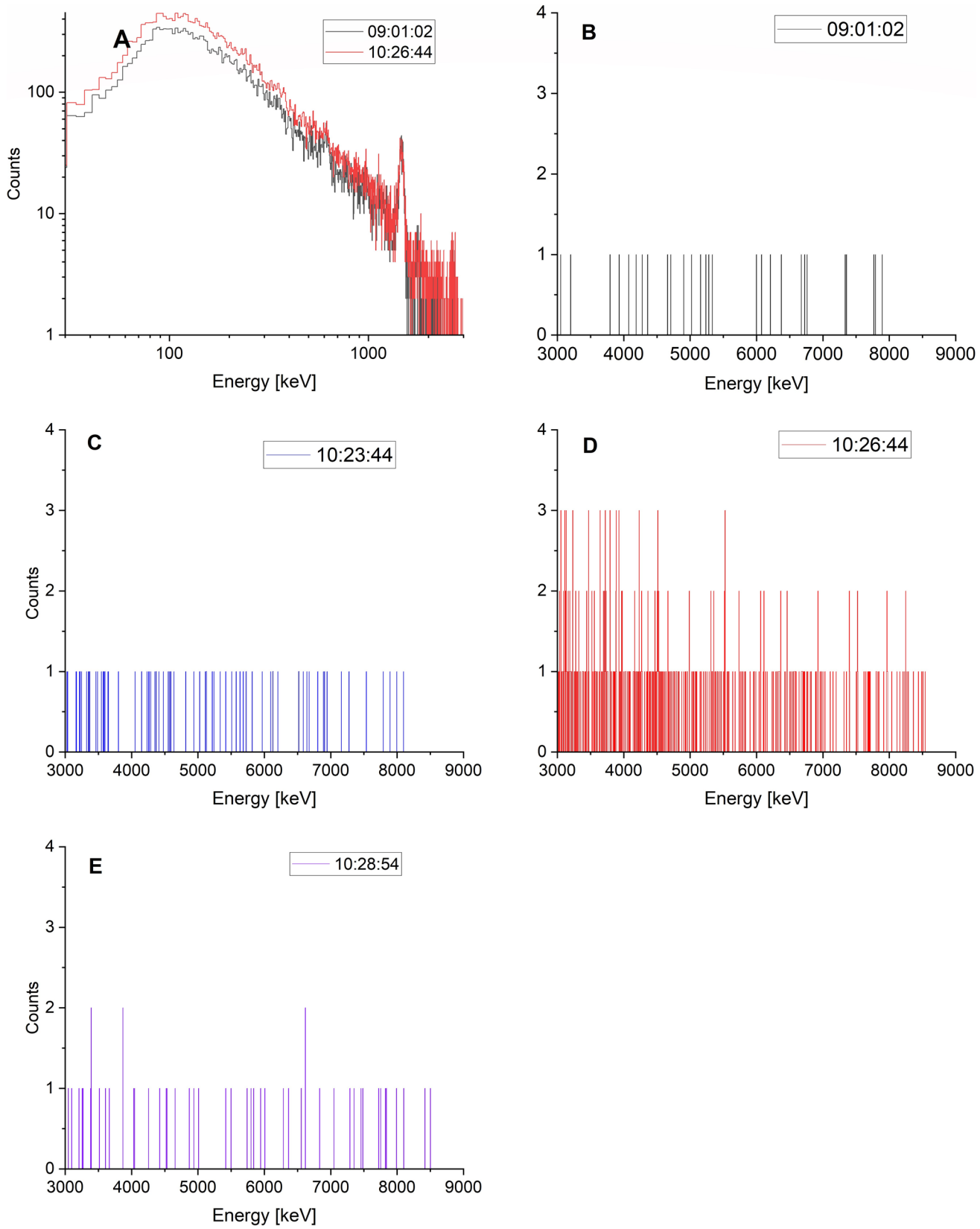
A
09:01:02
10:26:44
Counts
Energy [keV]
B
09:01:02
C
10:23:44
D
10:26:44
E
10:28:54

◂**Fig. 5** Ten second γ spectra from Detector 2. In Panel A low energy part of the spectra are shown taken at 09:01:02 and 10:26:44 UTC. In Panel B, high-energy part of the background radiation spectrum is shown with 28 counts, in Panel C, the peak of the first enhancement showing 74 counts, in Panel D, the peak of the second enhancement showing 374 counts and in Panel E, the peak of the possible third enhancement showing 51 counts

γ-ray spectrum analysis

When analyzing spectra, it should also be noted that detection efficiency in NaI(Tl) detectors is energy dependent with highest efficiency around 100–200 keV. At higher energies than this, the detection efficiency goes down quite fast. At the energies of a few MeVs and above, the detection efficiency does not decrease much, but it remains relatively constant despite the increasing γ-ray energy. This enhances the detection of low-energy γ rays compared to the detection of the high-energy γ rays. This difference in detection efficiency was not corrected here since the correction is dependent on the measurement geometry and the geometry in this case was not known.

Figure 5 shows a comparison of five 10-s. spectra from Detector 2 where the enhancements were observed to be strongest. We selected three time periods for comparison: (1) at 09:01:02 UTC when the radiation conditions were at background level, (2) at 10:23:44 UTC when the first enhancement peaked and (3) at 10:26:44 UTC at the peak of the second enhancement. Figure 5A shows a comparison of the low energy part of the spectrum between 09:01:02 and 10:26:44 UTC. A steady increase in the γ radiation throughout the energy range between 30—ca. 1000 keV was seen. This was believed to be caused by the bremsstrahlung of the RREA electrons (Babich et al. 2004). As electrons travel through air they slow down after interactions with atmospheric atoms. These interactions produce bremsstrahlung with a wide energy range.

Panels B, C, D and E show the high-energy part of the γ spectra from 3000 to 8800 keV. The observed γ-ray energies went up to the maximum energy of the detector systems. The background radiation in this part of the γ spectrum is very low as shown in Panel B where there is a total of 28 ± 5 counts from the bremsstrahlung from the secondary cosmic ray muons. The uncertainty shown here represents the variance of the Poisson distribution calculated as $N^{1/2}$. The muon flux can be considered as constant in the time scales used in this study. Panel C shows the high-energy part of the spectrum during the first enhancement where the number of high-energy γ rays was increased to 74 ± 9, which were 2.5 times higher than the background level taken 1.5 h before the first enhancement. Panel D shows the high-energy part of the spectrum at the peak of the second enhancement. The number of high-energy γ rays has increased further to 374 ± 19 counts which are 13.5 times higher than the background level. Panel E shows the high-energy γ spectrum from the possible third event. In this spectrum, 51 ± 7 counts were found, which is higher than the background spectrum used here, but the total counts in the high-energy part of the spectrum oscillated between 25 and 50 during the reference period from 9:00 to 9:02 UTC. Hence, the third enhancement remains speculative.

It has been proposed that the relativistic electrons can also cause nuclear reactions, for example in ^{14}N and ^{16}O (Enoto et al. 2017). ^{13}N, ^{14}N, ^{15}O and ^{16}O have rather complex nuclear structures where excitation would lead to the emission of multiple high-energy γ rays. Due to the low number of counts and poor energy resolution, clearly visible peaks or peak-like structures were not expected to be found in Panels C, D or E. Indeed, structures like these were not found in the spectra and no direct evidence of de-excitation of ^{13}N and ^{15}O was seen. The counts in the high-energy region originate from the tail of the bremsstrahlung continuum.

We studied more closely the γ spectrum from the second and stronger TGE. In total, 11 ten-second spectra from the starting time of 10:25:24 to 10:27:04 UTC were summed up to form one spectrum. For the background, we summed up 11 spectra from 09:00 to 09:02 UTC. The two summed spectra were then subtracted to see the net increase in γ radiation. Figure 6 shows resulted γ spectra where the bin size was increased from 5 keV per channel to 20 keV per channel to improve visualization. In Fig. 6, the maximum was reached between 100 and 200 keV. The enhancement produced γ rays from very low energies up to the maximum energy of the detector system at 8800 keV. The data from Detectors 1, 2 and 3 in Fig. 6 have been plotted into a log–log scale; above 200 keV, the data can be fitted with a straight line meaning that the data show a decreasing power law behavior. However, to resolve the true distribution of γ rays from RREA, the spectrum would have to be corrected for detection efficiency, but this could not be done since the detector was not calibrated for high energies. The spectral shape resembles closely the shape of γ spectra observed from bremsstrahlung reported in Wada et al. (2019) and Helmerich et al. (2024). Furthermore, Berge and Celestin (2019) calculated the theoretical photon spectrum created by an RREA and those spectra corresponded with the spectral shape observed in this study. The majority of the γ radiation in a TGE comes from the bremsstrahlung emitted by the slowing down of the relativistic electrons in the ongoing RREA inside the thundercloud. There was a minor increase in the 511 keV peak after the background subtraction. The washout of atmospheric dust and radon progenies after intense rain and wet snow could cause the increase in the NOR background which could, for example, enhance the peaks of ^{214}Bi and ^{40}K. The peaks belonging to NOR were not seen in any of the spectra in Fig. 6. Furthermore, the washout of radon progenies or atmospheric dust cannot

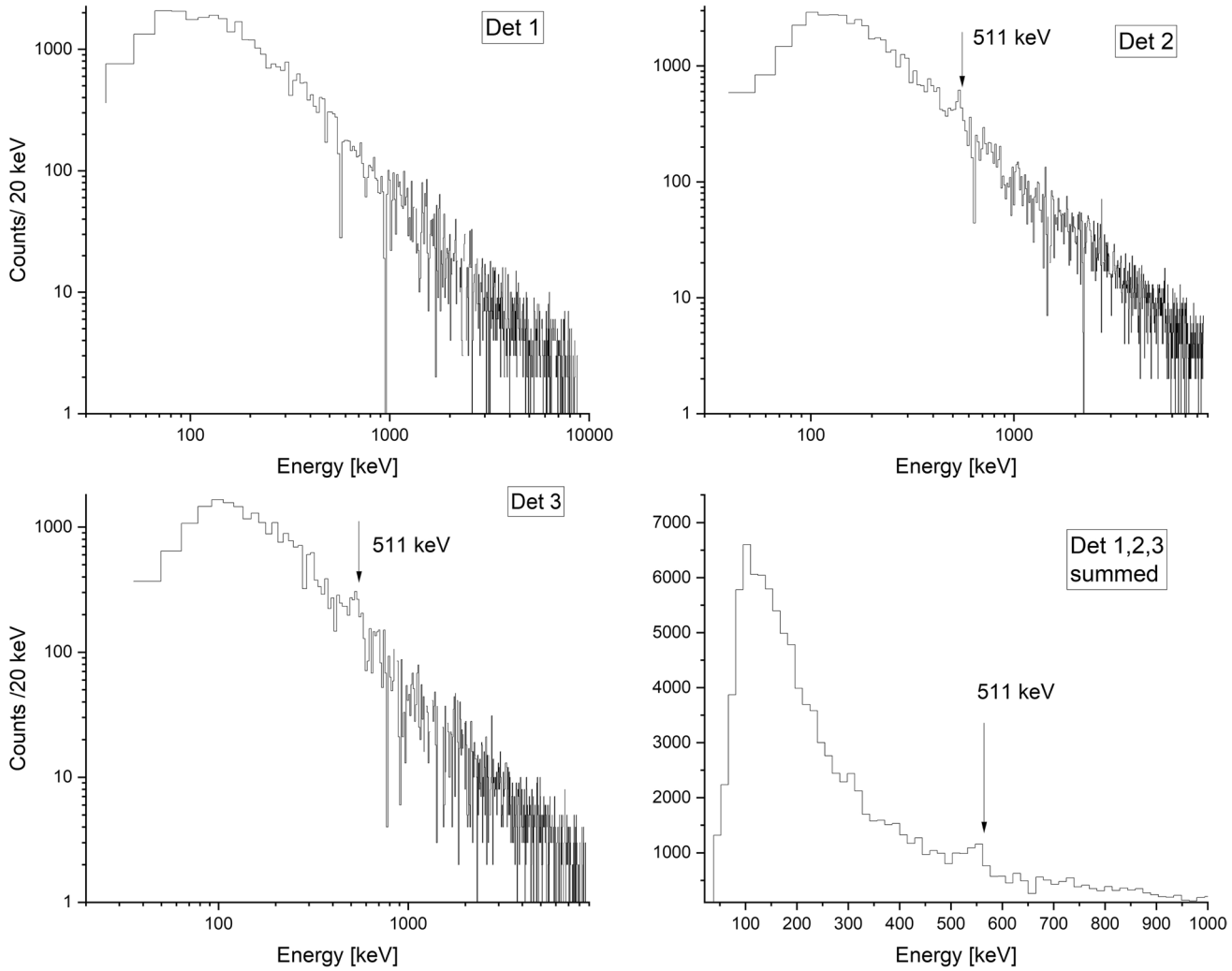

Fig. 6 Background subtracted gamma spectra from all detectors. The spectra produced by the second TGE look very similar to the predicted photon spectrum from RREAs. The small enhancement in 511 keV peak is marked with an arrow

explain the minor enhancement in the 511 keV peak seen in Detectors 2 and 3 and in the summed spectrum in Fig. 6 since NORs does not decay via $\beta+$ decay.

The main interaction modes of γ rays with matter below 1 MeV are the photoelectric affect and the Compton scattering. When the γ-ray energy is higher than 1022 keV, the pair production becomes possible, forming positron and electron pairs. The positrons collide with electrons creating two 511 keV γ rays. The pair production competes as an interaction mode with Compton scattering when the γ-ray energy is a few MeVs and it becomes the dominant interaction mode when the γ-ray energy is above 6–7 MeV (Knoll 2010). Hence, a small enhancement of the 511 keV annihilation peak can be expected. Such 511 keV annihilation peak enhancements have been observed in TGFs and in balloon missions sent inside a thundercloud (Briggs et al. 2010; Helmerich et al. 2024). The enhancements most likely originate from the pair production caused by high-energy photons and the subsequent annihilation of the positron. To study this enhancement, we plotted the time series of the count rates of the ten second spectra with 511 keV ± 20 keV energy window. Figure 7 shows clear increases in the count rates in all detectors. However, two things contributed to the 511 keV peak enhancement (1) possible increase in the β+ decays and (2) the increase caused by the bremsstrahlung continuum. We tried to estimate contribution from the bremsstrahlung and from the $\beta+$ decays. The total number of counts in the summed spectrum in Fig. 6 inside this energy window was about 1000 counts per channel, whereas the immediate channels below and above typically had about 800 counts per channel. Hence, a crude estimation can be made that in about 80% of the increase in the 511 keV peak originated from the bremsstrahlung and approximately 20% from the β+ decays caused by the pair production. This

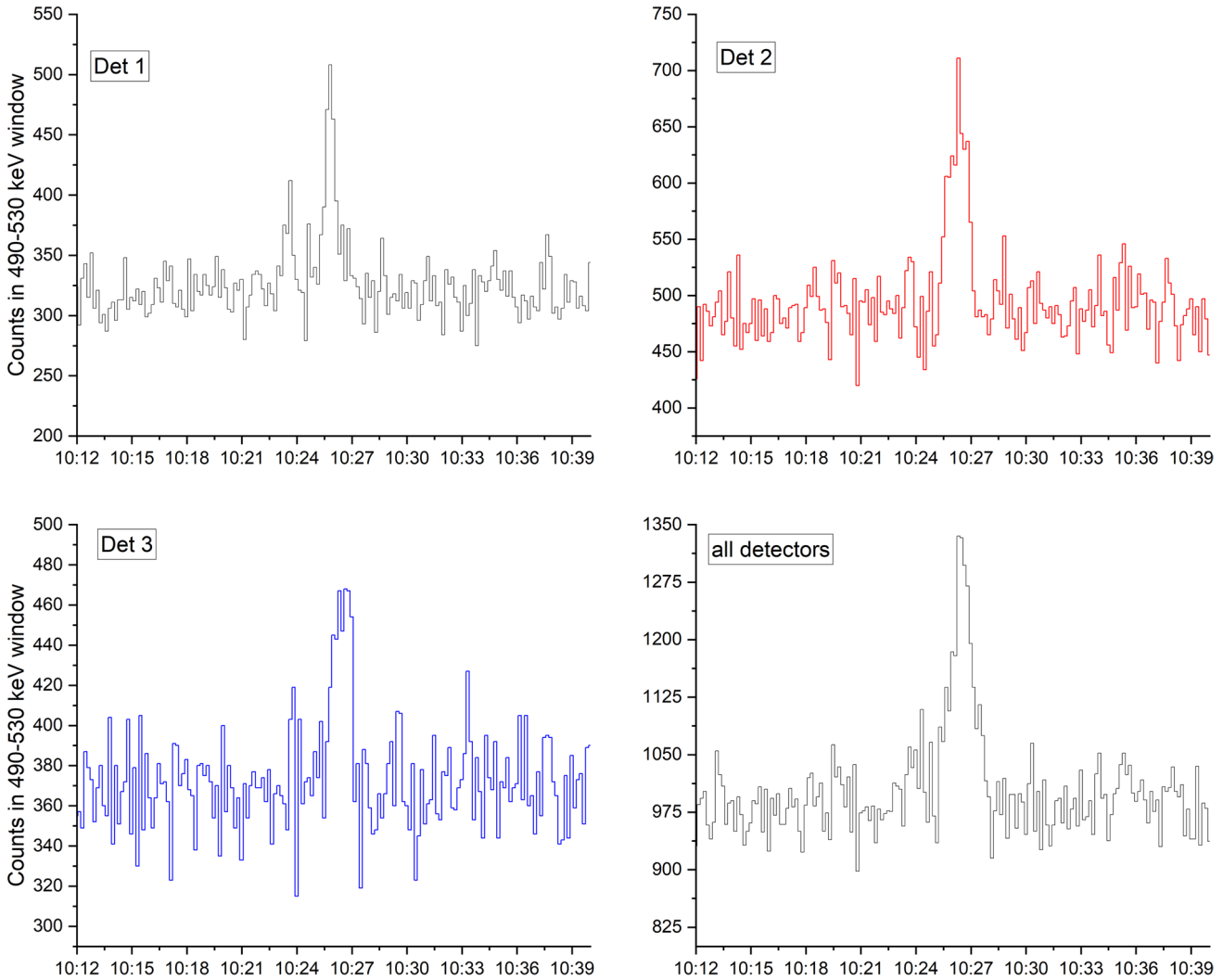

Fig. 7 Temporal behavior of count rates in the 511 ± 20 keV energy window

can be expected since the intensity of γ rays in high-energy region was low and the number of γ rays undergoing pair production was even lower.

The peak shapes in Fig. 7 corresponded to a very narrow beam of 511 keV γ rays where most of the annihilation γ rays are emitted in a forward direction straight from the cloud to the ground. Hence, the area emitting 511 keV γ rays was closely related to the size of the LPCR inside the thundercloud. Enoto et al. (2017) detected a delayed decaying count rate in the 511 keV peak after the TGE had terminated. In the present study, no delayed decrease in the count rates was observed after the termination of the second TGE at 10:27:04 UTC.

A TGE requires certain conditions to occur. A tripole structure inside a thundercloud is needed and the LPCR needs to be close to the ground (cloud base at ~ 500 m or below) to allow detection. The potential difference inside the thundercloud must be above the threshold potential. A TGE is born when RREA accelerates the electrons close to relativistic energies. The accelerated electrons create the γ radiation and particle fluxes that can be detected by ground-level detector systems. As the electrons in RREA interact with atmospheric atoms, they created a flux of bremsstrahlung with a wide energy range from 100 keV up to the maximum of the detector system used in this study. Here, two different TGEs were observed which lasted from 50 to 100 s and were terminated suddenly by lightning. In this study, the TGEs were observed at low altitude and in high latitude in spring conditions. The thundercloud having the RREA did brought about winter conditions with a low surface temperature and snow. In a balloon flight conducted in Mississippi, the TGF events were detected to occur at the freezing altitude (Helmerich et al., 2023). The original seed for RREAs comes from cosmic-ray induced atmospheric ionization. Ionized electrons are accelerated to relativistic energies by the electric field inside a thundercloud. The

highest intensity of bremsstrahlung was at lower energies below 1000 keV and the number of bremsstrahlung photons decreased with a power law function toward high energies. The bremsstrahlung contributed to a wide energy range including the 511 keV peak. However, the 511 keV peak enhancement cannot be fully explained by the bremsstrahlung, but there was also a minor increase possibly caused by increased $\beta+$ decay from high-energy photon pair production. The enhancement of the 511 keV peak was limited to the passing of the LPCR in the thundercloud and no delayed component in the count rate was observed.

Conclusions

Rare high-latitude, low-altitude observations of two Thunderstorm Ground Enhancements (TGE) were made for the first time in Finland. The observation were made in the Municipality of Vantaa on May 17th, 2020 between 10:20 and 10:30 UTC when a storm front containing a large amount of moisture and cold air moved across the Baltic Sea to the mainland Finland. The local weather conditions favored the detection of TGEs since the cloud base was at 640 m above ground level. The TGE detections were made with high efficiency NaI(Tl) detectors with two- and ten-second data acquisition times. The detectors observed radiation in a broad energy range from 30 keV to 8800 keV. Two TGE events were detected with certainty and an uncertain small third event. The first TGE lasted ~ 50 s and the γ-ray count rates were observed to increase by 5–12%. The first TGE was terminated by an in-cloud lightning strike with a 3-kA peak current. The first event was followed by a break of 86-104 s. when the radiation levels went back to background level. After the break, a second and stronger TGE event was observed which lasted ~ 100 s. and the γ-ray count rates increased by 20–50%. The second event was also terminated by an in-cloud lightning with a 29-kA peak current. The horizontal dimension of the LPCR in the second TGE event was estimated by using the prevailing wind conditions and the duration of the peak phase in the high-energy γ count rate. The horizontal size was estimated to be around 500 m in diameter with an upper limit at 1000 m in diameter. A closer look was taken at the γ spectra recorded during the second TGE event. The highest increase in the γ spectrum was observed of energies around 200 keV. Above 200 keV the amount of radiation decreased as a function of energy where the decrease followed a power law. The maximum energy of the γ rays reached the upper limit of our detector systems at 8800 keV. The γ-spectrum shape corresponded to the previously observed bremsstrahlung emission spectra from RREA events inside thunderclouds. In the background-subtracted γ spectra, we observed a minor increase in the 511 keV peak suggesting that the high-energy bremsstrahlung also produced positrons ($\beta+$ particles) possibly via pair production which subsequently produced 511 keV annihilation γ rays. This is understandable since pair production becomes the dominant interaction mode when γ rays with several MeVs in energy interact with matter. The delayed decay of count rates in this energy window could suggest the presence of atmospheric photonuclear reactions producing radioactive isotopes, for example, $^{14}\mathrm{N}+\gamma \rightarrow {}^{13}\mathrm{N}+\mathrm{n}$ which decay via $\beta+$ decay producing 511 keV γ rays and hence delaying the decrease of the 511 keV count rate. The count rates of the 511 ± 20 keV energy window matched start and end times of the second TGE event and no delayed decay was observed.

Acknowledgements APL thanks Risto Leppänen for the help in building the time series information.

Funding The authors of this article have not received any funding from any other organisations other than their own.

Declarations

Conflict of Interest The authors declare that they have no conflict of interest.

References

Babich LP, Donskoy EN, Kutsyk IM, Roussel-Dupré RA (2004) Characteristics of a relativistic electron avalanche in air. Dokl Phys 49:35–38

Bazilevskaya GA, Usoskin IG, Flückiger EO, Harrison RG, Desorgher L, Bütikofer R, Krainev MB, Makhmutov VS, Stozhkov YI, Svirzhevskaya AK, Svirzhevsky NS, Kovaltsov GA (2008) Cosmic ray induced ion production in the atmosphere. Space Sci Rev 137:149–173

Berge N, Celestin S (2019) Constraining downward terrestrial gamma ray flashes using ground-based particle detector arrays. Geo Phys Res Lett 46:8424–8430

Bowers GS, Smith DM, Martinez-McKinney GF, Kamogawa M, Cummer SA, Dwyer JR, Wang D, Stock M, Kawasaki Z (2017) Gamma ray signatures of neutrons from a terrestrial gamma ray flash. Geophys Res Lett 44(19):10063–10070

Briggs MS, Fishman GJ, Connaughton V, Bhat PN, Paciesas WS, Preece RD, Wilson-Hodge C, Chaplin VL, Kippen RM, von Kienlin A, Meegan CA, Bissaldi E, Dwyer JR, Smith DM, Holzworth RH, Grove JE, Chekhtman A (2010) First results on terrestrial

gamma ray flashes from the Fermi Gamma-ray Burst Monitor. J Geophys Res 115:A07323
Chilingarian A (2013) Thunderstorm ground enhancements (TGES)—new high-energy phenomenon originated in the terrestrial atmosphere. J Phys: Conf Ser 409:012019
Chilingarian A (2014) Thunderstorm ground enhancements—model and relation to lightning flashes. J Atm Sol Terr Phys 107:68–76
Chilingarian A (2023) thunderstorm ground enhancements measured on aragats and progress of high-energy physics in the atmosphere. Atmosphere 14:300
Chilingarian A, Hovsepyan G, Karapetyan T, Kozliner L, Chilingaryan S, Pokhsraryan D, Sargsyan B (2022) The horizontal profile of the atmospheric electric fields as measured during thunderstorms by the network of NaI spectrometers located on the slopes of Mt. Aragats. J Instrum 17:P10011
Chubenko AP, Antonova VP, Kryukov SY, Piscal VV, Ptitsyn MO, Shepetov AL, Vildanova LI, Zybin KP, Gurevich AV (2000) Intensive X-ray emission bursts during thunderstorms. Phys Lett A 275:90–100
Dwyer JR (2003) A fundamental limit on electric fields in air. Geophys Res Lett 30(20):2055
Dwyer JR, Smith DM, Cummer SA (2012) High-energy atmospheric physics: terrestrial gamma-ray flashes and related phenomena. Space Sci Rev 173:133–196
Eack KB, Beasley WH, Rust WD, Marshall TC, Stolzenburg M (1996) Initial results from simultaneous observation of X rays and electric fields in a thunderstorm. J Geophys Res 101:29637–29640
Enoto T, Wada Y, Furuta Y, Nakazawa K, Yuasa T, Okuda K, Makishima K, Sato M, Sato Y, Nakano T, Umemoto D, Tsuchiya H (2017) Photonuclear reactions triggered by lightning discharge. Nature 551:481–484
Finnish Meteorological Institute (FMI) (2023) Finnish Meteorological Institute Open Data, Finnish government. Accessed February 2023. https://en.ilmatieteenlaitos.fi/open-data
Gurevich AV, Chubenko AP, Karashtin AN, Mitko GG, Naumov AS, Ptitsyn MO, Ryabov VA, Shepetov AL, Shlyugaev YuV, Vildanova LI, Zybin KP (2011) Gamma-ray emission from thunderstorm discharges. Phys Lett A 375(15):1619–1625
Helmerich C, Mckinney T, Cavanaugh E, Dangelo S (2024) TGFs, gamma-ray glows and direct lightning strike radiation observed during a single flight of a balloon-borne gamma-ray spectrometer. Earth Space Sci 11(2):e2023EA003317
Hisadomi S, Nakazawa K, Wada Y, Tsuji Y, Enoto T, Shinoda T, Morimoto T, Nakamura Y, Yuasa T, Tsuchiya H (2021) Multiple gamma-ray glows and a downward TGF observed from nearby thunderclouds. J Geophys Res: Atmos 126:s
Holm P, Peräjärvi K, Sihvonen A-P, Siiskonen T, Toivonen T (2013) Neutron detection with a NaI spectrometer using high-energy photons. Nucl Inst Methods Phys Res A 697:59–63
Knoll GF (2010) Radiation interactions. In: Radiation Detection and Measurement, 4th edn., John Wiley and Sons Inc., p 48
Köhn C, Ebert U (2014) Angular distribution of Bremsstrahlung and of positrons for calculations of terrestrial gamma-ray flashes and positron beams. Atmos Res 135–136:432–465
Kolmašová I, Santolík O, Šlegl J, Popová J, Sokol Z, Zacharov P, Ploc O, Diendorfer G, Langer R, Lán R, Strhárský I (2022) Continental thunderstorm ground enhancement observed at an exceptionally low altitude. Atmos Chem Phys 22:7959–7973
Kuettner J (1950) The electrical and meteorological conditions inside thunderclouds. J Meteorol 7:322–332
Maia JM, Curado da Silva RM, Mingacho J (2024) Evaluation of effective dose for gamma-rays of terrestrial gamma-ray flashes in aviation: spectral and atmosphere effects. Rad Phys and Chem 215:111332
Mäkelä A, Saltikoff E, Julkunen J, Juga I, Gregow E, Niemelä S (2013) Cold-season thunderstorms in Finland and their effect on aviation safety. BAMS 94(6):847–858
Mäkelä A, Enno S-E, Haapalainen J (2014) Nordic lightning information system: thunderstorm climate of northern Europe for the period 2002–2011. Atmos Res 139:46–61
Mäkelä A, Laurila TK, Haapalainen J, Halabi T, (2017) Lightning Observations in Finland, 2016. Reports 2017:8. Finnish Meteorological Institute, Helsinki, p 51
Marisaldi M, Argan A, Trois A, Giuliani A, Tavani M, Labanti C, Fuschino F, Bulgarelli A, Longo F, Barbiellini G, Del Monte E, Moretti E, Trifoglio M, Costa E, Caraveo P, Cattaneo PW, Chen A, D'Ammando F, De Paris G, Di Cocco G, Di Persio G, Donnarumma I, Evangelista Y, Feroci M, Ferrari A, Fiorini M, Froysland T, Galli M, Gianotti F, Lapshov I, Lazzarotto F, Lipari P, Mereghetti S, Morselli A, Pacciani L, Pellizzoni A, Perotti F, Picozza P, Piano G, Pilia M, Prest M, Pucella G, Rapisarda M, Rappoldi A, Rubini A, Sabatini S, Soffitta P, Striani E, Vallazza E, Vercellone S, Vittorini V, Zambra A, Zanello D, Antonelli LA, Colafrancesco S, Cutini S, Giommi P, Lucarelli F, Pittori C, Santolamazza P, Verrecchia F, Salotti L (2010) Gamma-ray localization of terrestrial gamma-ray flashes. Phys Rev Lett 105(21):128501
Marisaldi M, Fuschino F, Tavani M, Dietrich S, Price C, Galli M, Pittori C, Verrecchia F, Mereghetti S, Cattaneo PW, Colafrancesco S, Argan A, Labanti C, Longo F, Del Monte E, Barbiellini G, Giuliani A, Bulgarelli A, Campana R, Chen A, Gianotti F, Giommi P, Lazzarotto F, Morselli A, Rapisarda M, Rappoldi A, Trifoglio M, Trois A, Vercellone S (2014) Properties of terrestrial gamma ray flashes detectedby AGILE MCAL below 30 MeV. J Geophys Res Space Phys 119:1337–1355
National Oceanic and Atmosphere Administration, National Weather Service (NWS) website https://www.weather.gov/mlb/lightning_facts. Accessed 12.4.2024
Paatero J, Hatakka J (1999) Wet deposition efficiency of short-lived radon-222 progeny in central Finland. Boreal Environ Res 4(4):285–293
Parks GK, Mauk BH, Spiger R, Chin J (1981) X-ray enhancements detected during thunderstorm and lightning activities. Geophys Res Lett 8:1176–1179
Smith DM, Lopez LI, Lin RP, Barrington-Leigh CP (2005) Terrestrial gamma-ray flashes observed up to 20 MeV. Science 307:1085–1088
Tavani M, Marisaldi M, Labanti C, Fuschino F, Argan A, Trois A, Giommi P, Colafrancesco S, Pittori C, Palma F, Trifoglio M, Gianotti F, Bulgarelli A, Vittorini V, Verrecchia F, Salotti L, Barbiellini G, Caraveo P, Cattaneo PW, Chen A, Contessi T, Costa E, D'Ammando F, Del Monte E, De Paris G, Di Cocco G, Di Persio G, Donnarumma I, Evangelista Y, Feroci M, Ferrari A, Galli M, Giuliani A, Giusti M, Lapshov I, Lazzarotto F, Lipari P, Longo F, Mereghetti S, Morelli E, Moretti E, Morselli A, Pacciani L, Pellizzoni A, Perotti F, Piano G, Picozza P, Pilia M, Pucella G, Prest M, Rapisarda M, Rappoldi A, Rossi E, Rubini A, Sabatini S, Scalise E, Soffitta P, Striani E, Vallazza E, Vercellone S, Zambra A, Zanello D (2011) Terrestrial gamma-ray flashes as powerful particle accelerators. Phys Rev Lett 106(1):018501
Tavani M, Argan A, Paccagnella A, Pesoli A, Palma F, Gerardin S, Bagatin M, Trois A, Picozza P, Benvenuti P, Flamini E, Marisaldi M, Pittori C, Giommi P (2013) Possible effects on avionics induced by terrestrial gamma-ray flashes. Nat Hazards Earth Syst Sci 13:1127–1133
Torii T, Takeishi M, Hosono T (2002) Observation of gamma-ray dose increase associated with winter thunderstorm and lightning activity. J Geophys Res 107(D17):4324
Torii T, Sugita T, Tanabe S, Kimura Y, Kamogawa M, Yajima K, Yasuda H (2009) Gradual increase of energetic radiation associated with thunderstorm activity at the top of Mt. Fuji. Geophys Res Lett 36:L13804
Torii T, Sugita T, Kamogawa M, Watanage Y, Kusunoki K (2011) Migrating source of energetic radiation generated by thunderstrom activity. Geophys Res Lett 38:L24891

Usoskin I, Poluianov S (2024) Cosmic-ray-induced processes in the atmosphere. Ref Module Earth Syst Environ Sci. https://doi.org/10.1016/B978-0-323-99762-1.00131-5

Wada Y, Enoto T, Nakamura Y, Furuta Y, Yuasa T, Nakazawa K, Morimoto T, Sato M, Matsumoto T, Yonetoku D, Sawano T, Sakai H, Kamogawa M, Ushio T, Makishima K, Tsuchiya H (2019) Gamma-ray glow preceding downward terrestrial gamma-ray flash. Comm Phys 2:67

Wilson CTR (1925) The Acceleration of β-particles in Strong Electric Fields such as those of Thunderclouds. Proc Camb Philol Soc 22:534–538